



HAL
open science

Redox modifications of cysteine-containing proteins, cell cycle arrest and translation inhibition: Involvement in vitamin C-induced breast cancer cell death

Nadine El Banna, Elie Hatem, Amélie Heneman-Masurel, Thibaut Léger, Dorothee Baille, Laurence Vernis, Camille Garcia, Sylvain Martineau, Corinne Dupuy, Stéphan Vagner, et al.

► **To cite this version:**

Nadine El Banna, Elie Hatem, Amélie Heneman-Masurel, Thibaut Léger, Dorothee Baille, et al.. Redox modifications of cysteine-containing proteins, cell cycle arrest and translation inhibition: Involvement in vitamin C-induced breast cancer cell death. *Redox Biology*, 2019, 26, pp.101290. 10.1016/j.redox.2019.101290 . hal-02389344

HAL Id: hal-02389344

<https://cnrs.hal.science/hal-02389344>

Submitted on 2 Dec 2019

HAL is a multi-disciplinary open access archive for the deposit and dissemination of scientific research documents, whether they are published or not. The documents may come from teaching and research institutions in France or abroad, or from public or private research centers.

L'archive ouverte pluridisciplinaire **HAL**, est destinée au dépôt et à la diffusion de documents scientifiques de niveau recherche, publiés ou non, émanant des établissements d'enseignement et de recherche français ou étrangers, des laboratoires publics ou privés.



Research Paper

Redox modifications of cysteine-containing proteins, cell cycle arrest and translation inhibition: Involvement in vitamin C-induced breast cancer cell death



Nadine El Banna^a, Elie Hatem^a, Amélie Heneman-Masurel^a, Thibaut Léger^b, Dorothée Baille^a, Laurence Vernis^a, Camille Garcia^b, Sylvain Martineau^a, Corinne Dupuy^c, Stéphan Vagner^a, Jean-Michel Camadro^b, Meng-Er Huang^{a,*}

^a Institut Curie, PSL Research University, CNRS UMR 3348, Université Paris-Sud, Université Paris-Saclay, Orsay, France

^b Institut Jacques Monod, CNRS UMR 7592, Mass Spectrometry Laboratory, Université Paris Diderot, Paris, France

^c Institut Gustave Roussy, CNRS UMR 8200, Université Paris-Sud, Villejuif, France

ARTICLE INFO

Keywords:

Vitamin C
Ascorbic acid
Dehydroascorbic acid
Breast cancer
Oxidative stress
Redoxome

ABSTRACT

Vitamin C (VitC) possesses pro-oxidant properties at high pharmacologic concentrations which favor repurposing VitC as an anti-cancer therapeutic agent. However, redox-based anticancer properties of VitC are yet partially understood. We examined the difference between the reduced and oxidized forms of VitC, ascorbic acid (AA) and dehydroascorbic acid (DHA), in terms of cytotoxicity and redox mechanisms toward breast cancer cells. Our data showed that AA displayed higher cytotoxicity towards triple-negative breast cancer (TNBC) cell lines *in vitro* than DHA. AA exhibited a similar cytotoxicity towards non-TNBC cells, while only a minor detrimental effect on noncancerous cells. Using MDA-MB-231, a representative TNBC cell line, we observed that AA- and DHA-induced cytotoxicity were linked to cellular redox-state alterations. Hydrogen peroxide (H₂O₂) accumulation in the extracellular medium and in different intracellular compartments, and to a lesser degree, intracellular glutathione oxidation, played a key role in AA-induced cytotoxicity. In contrast, DHA affected glutathione oxidation and had less cytotoxicity. A “redoxome” approach revealed that AA treatment altered the redox state of key antioxidants and a number of cysteine-containing proteins including many nucleic acid binding proteins and proteins involved in RNA and DNA metabolisms and in energetic processes. We showed that cell cycle arrest and translation inhibition were associated with AA-induced cytotoxicity. Finally, bioinformatics analysis and biological experiments identified that peroxiredoxin 1 (*PRDX1*) expression levels correlated with AA differential cytotoxicity in breast cancer cells, suggesting a potential predictive value of *PRDX1*. This study provides insight into the redox-based mechanisms of VitC anticancer activity, indicating that pharmacologic doses of VitC and VitC-based rational drug combinations could be novel therapeutic opportunities for triple-negative breast cancer.

1. Introduction

Reactive oxygen species (ROS) homeostasis and intracellular reductive/oxidative (redox) dynamics play a key role in regulating cell viability or death. Mounting evidence has established that defects in redox signaling and oxidative stress are at the crux of various pathological processes. Notably, one of the significant features of cancer cells, when compared to their normal counterparts, is a persistent pro-oxidative state. In cancer cells, cellular events such as activation of oncogenes, aberrant metabolic stress and mitochondrial dysfunction can

increase ROS levels, leading to intrinsic oxidative stress [1,2]. Therefore, the administration of a ROS-generating agent or antioxidant inhibitor could increase ROS levels to a threshold that is incompatible with viability, selectively and preferentially affecting cancer cells [1–3].

Vitamin C (VitC) is an essential nutrient used as a co-factor by numerous biosynthetic enzymes. It exists in the parental reduced form or ascorbic acid (AA, or AsC₂) and the oxidized forms, encompassing the ascorbate radical (Asc^{•-}) and the dehydroascorbic acid (DHA). At physiological pH (7.0), the dominant species for VitC is ascorbate

* Corresponding author. CNRS UMR3348, Institut Curie, Bâtiment 110, Centre Universitaire, 91405, Orsay, France.

E-mail address: meng-er.huang@curie.fr (M.-E. Huang).

<https://doi.org/10.1016/j.redox.2019.101290>

Received 27 June 2019; Received in revised form 28 July 2019; Accepted 31 July 2019

Available online 02 August 2019

2213-2317/ © 2019 The Authors. Published by Elsevier B.V. This is an open access article under the CC BY-NC-ND license (<http://creativecommons.org/licenses/by-nc-nd/4.0/>).

Abbreviations

AA	ascorbic acid
BrdU	5-bromo-2'-deoxy-uridine
DAVID	Database for Annotation, Visualization and Integrated Discovery
DHA	dehydroascorbic acid
DTT	dithiothreitol
GLUT1	glucose transporter 1
GO	Gene ontology
IPA	Ingenuity Pathways Analysis software

LC-MS/MS	liquid-chromatography tandem mass spectrometry
MTT	3-(4,5-dimethylthiazol-2-yl)-2,5-diphenyltetrazolium bromide
NAC	N-acetyl-L-cysteine
NEM	N-ethylmaleimide
PI	propidium iodide
SVCT	sodium-dependent vitamin C transporter
TCA	trichloroacetic acid
TNBC	triple-negative breast cancer
VitC	vitamin C

monoanion (AscH^- , 99.9%), with low concentrations of AscH_2 (0.1%) and ascorbate dianion (Asc^{2-} , 0.005%) [4]. The ability to donate one or two electrons makes ascorbate (AscH^-) an excellent reducing agent and antioxidant. At millimolar levels (pharmacologic concentrations), AA becomes a ROS-generating molecule. In fact, a small portion of AA, via the ascorbate dianion (Asc^{2-}), can undergo limited pH-dependent auto-oxidation that can lead to superoxide anion ($\text{O}_2^{\cdot-}$) formation according to the following reaction: $\text{Asc}^{2-} + \text{O}_2 \rightarrow \text{Asc}^- + \text{O}_2^{\cdot-}$ [4,5]. Superoxide anions subsequently dismutate to produce H_2O_2 ($\text{O}_2^{\cdot-} + \text{O}_2^{\cdot-} + 2\text{H}^+ \rightarrow \text{H}_2\text{O}_2 + \text{O}_2$). Importantly, in the presence of redox active metal ions, AA oxidation is further accelerated and amplified as ascorbate (AscH^-) can exert an additional pro-oxidant effect. AscH^- donates one electron to metals, that can reduce ferric (Fe^{3+}) to ferrous (Fe^{2+}) iron for example, while being oxidized to ascorbate radical ($\text{AscH}^- + \text{Fe}^{3+} \rightarrow \text{Asc}^{\cdot-} + \text{Fe}^{2+} + \text{H}^+$). Fe^{2+} can readily react with O_2 , reducing it to superoxide anion ($\text{O}_2 + \text{Fe}^{2+} \rightarrow \text{O}_2^{\cdot-} + \text{Fe}^{3+}$), which in turn dismutates to H_2O_2 and O_2 [4,5]. These mechanisms act to produce a high flux of H_2O_2 at pharmacologic concentrations of AA. In a classic Fenton reaction, Fe^{2+} reacts with H_2O_2 to generate Fe^{3+} and the highly reactive hydroxyl radical.

H_2O_2 generated in the extracellular medium or extracellular fluids appears to be the central player for pro-oxidant properties of AA at pharmacologic concentrations, achievable in cell culture experiments, and *in vivo* by intravenous administration. Extracellular H_2O_2 readily diffuses into cells; if not removed, it can lead to oxidative damage to proteins, lipids, and DNA. On the other hand, it is expected that AA, upon import through plasma membranes via sodium-dependent VitC transporters (SVCTs), can generate intracellular H_2O_2 directly by the same metals-catalyzed reactions described above. In accordance, AA cytotoxicity was observed in a number of studies *in vitro* and *in vivo* models on cancer cells from different origins without adversely affecting normal cells [6–8]. Such cytotoxicity was also dependent on redox metal supply such as iron [9]. VitC anticancer effects driven by its DHA form were also reported [10]. Yun et al. observed that VitC was oxidized to DHA in cell culture media lacking reducing agents, and was subsequently imported into human colon cancer cells harboring oncogenic *KRAS* or *BRAF* mutations by overexpressed GLUT1 glucose transporter. Following import, DHA is reduced to AA at the expense of glutathione (GSH) and NADPH. Increased DHA uptake leads to GSH oxidation, thus indirectly promoting endogenous ROS accumulation and specific inactivation of glyceraldehyde 3-phosphate dehydrogenase (GAPDH), and consequently, impairing glycolysis and inducing cancer cell death [10].

Several studies addressed the question regarding VitC selective cytotoxicity toward cancer cell lines. Differential ability to metabolize H_2O_2 between normal and pancreatic cancer cells were shown to be determinant in AA effect on pancreatic cancer cells while sparing normal ones *in vitro* and *in vivo* [11]. In addition, a positive correlation between the sodium-dependent VitC transporter 2 (SVCT2) expression and AA cytotoxicity were reported in breast cancer cells, cholangiocarcinoma cell lines and patient-derived xenografts [12–14]. Interestingly, a recent study showed that non-small-cell lung cancer and

glioblastoma cells are selectively sensitive to AA due to their altered redox-active iron metabolism, resulted from altered mitochondrial oxidative metabolism and increased levels of $\text{O}_2^{\cdot-}$ and H_2O_2 [15]. The same team found similar benefits of pharmacological ascorbate in preclinical models of fibrosarcoma and liposarcoma [16]. Finally, different energy metabolisms between cancer and normal cells, known as the Warburg effect where cancer cells strongly depend on glycolysis for their energy and ATP production, render cancer cells far more vulnerable to glycolysis impairment by VitC than their normal counterparts [10,17,18].

Pharmacologic dose of AA enhanced chemosensitivity of ovarian cancer to carboplatin and paclitaxel and reduced toxicity of chemotherapy in mouse models [19]. AA also enhanced sensitivity to ionizing radiation by increasing H_2O_2 -mediated DNA damage in pancreatic cancer model [20,21], and in prostate cancer cells while sparing normal cells from radiotoxicity [22]. Clinical studies revealed that pharmacologic doses of AA were well tolerated and increased the efficacy of conventional radio-chemotherapy in non-small-cell lung cancer and glioblastoma patients [15], and in pancreatic cancer patients [23].

These recent studies reflect a regained interest in VitC anticancer activity. However, VitC redox-based anticancer mechanisms warrant further investigation. Notably, which form of VitC exhibits the higher anticancer activity? Is this effect cell-type dependent? What are the factors that condition cellular sensitivity to VitC? What are the key intermediates (H_2O_2 or GSH oxidation) that lead to cell death? And which proteins or pathways are key targets of VitC-mediated oxidation? In this study we provide answers to these questions using breast cancer model.

2. Materials and methods

2.1. Cell culture

Triple-negative breast cancer (TNBC) cell lines MDA-MB-231 and HTB-26, human umbilical vein endothelial cells (HUVEC) and human dermal fibroblasts (PCS-201-012) were purchased from American Type Culture Collection. Human mammary epithelial cells (HMEC) were purchased from Lonza. Additional breast cancer cell lines were obtained from the Translational Research Department of the Institut Curie (Paris, France). MDA-MB-231, MDA-MB-468, MDA-MB-436, BT-549, HCC-1937, BT-20, MDA-MB-453, MDA-MB-134, MDA-MB-415, HUVEC and fibroblasts cells were grown in DMEM (Eurobio) supplemented with 10% FBS, 2 mM L-glutamine, 1X non-essential amino acids, 1 mM sodium pyruvate and 100 U/ml penicillin and 100 µg/ml streptomycin. HCC-1187, HCC-1954, T47D, HCC-1428 were grown in RPMI medium supplemented with 10% FBS, 2 mM L-glutamine 100 U/ml penicillin and 100 µg/ml streptomycin. HMEC were grown in mammary epithelial basal medium (MEBM) supplemented with MEGM SingleQuots (Lonza) (containing bovine pituitary extract, hydrocortisone, hEGF, insulin and gentamicin/amphotericin-B), 10% FBS and 100 U/ml penicillin and 100 µg/ml streptomycin. Cells are incubated in humidified atmosphere at 37 °C with 5% CO_2 in air and were routinely checked for the absence

of mycoplasma. Cell lines were authenticated using standard DNA microsatellite short tandem repeat (STR) method.

2.2. Drugs and reagents

L-ascorbic acid (AA), L-dehydroascorbic acid (DHA), N-ethylmaleimide (NEM), crystal violet, N-acetyl-L-cysteine (NAC), glutathione, DMSO, dithiothreitol (DTT), hydrogen peroxide (H_2O_2), catalase, diamide, trichloroacetic acid (TCA) and cycloheximide were purchased from Sigma-Aldrich. 3-(4,5-dimethylthiazol-2-yl)-2,5-diphenyltetrazolium bromide (MTT), 6-carboxy-2',7'-dichlorodihydrofluorescein diacetate (carboxy- H_2DCFDA), 5-bromo-2'-deoxy-uridine (BrdU) and propidium iodide (PI) were from Thermo Fisher Scientific. The following antibodies were used: anti-PRDX3 (Abcam), anti-GFP (Life Technologies), anti- β -actin (Sigma-Aldrich), anti-PRDX1 (Cell Signaling Technology), FITC Mouse anti-BrdU (BD Biosciences).

2.3. ROS assessment, H_2O_2 detection and H_2O_2 quantification

General ROS were assessed using carboxy- H_2DCFDA staining and a FACSCalibur flow cytometer (Becton Dickinson) and data were analyzed using Flowjo software. For compartment-specific H_2O_2 detection, mammalian expression vectors encoding HyPer targeted to nucleus (with a nuclear localization signal), and mitochondria (with a mitochondrial matrix localization signal) were purchased from Evrogen. HyPer targeted to the cytosol with a nuclear export signal and HyPer targeted to the membrane using the membrane-targeting signal in protein GAP-4 were constructed in our laboratory. Cells were transfected with HyPer expressing vectors using jetPRIME reagents (Polyplus Transfection). Further experiments were performed 24 h after transfection. Analyses of oxidized and reduced forms of sensor by redox Western blot were performed according to Ref. [24]. H_2O_2 concentration in the medium was quantified using the Amplex Red Hydrogen Peroxide/Peroxidase Assay Kit (Thermo Fisher Scientific). The fluorescence was measured in a microplate reader (Victor3; PerkinElmer). H_2O_2 concentration in the growth medium (μM) was quantified using H_2O_2 standard calibration curves.

2.4. Quantitative redoxome analysis

Cells were subjected to different treatments and proteins were extracted. Purification of these proteins was performed according to a published protocol with slight modifications [25]. Protein digests were analyzed in triplicate with an Orbitrap Fusion Tribrid equipped with an EASY-Spray ion source. Label-free liquid-chromatography tandem mass spectrometry (LC-MS/MS) acquisition was performed. Peptides from MS/MS data were processed with Proteome Discoverer Software (v 2.1) using Sequest search node. All results were 1% FDR filtered before exporting. The resulting files were imported into Progenesis-Qi software for report edition. Variations of protein abundance were considered as significant if their Anova P values were < 0.05 . Details of the protocol and analysis are described in Supplementary Materials and Methods and Supplementary Fig. 1. The proteomics data have been deposited to the ProteomeXchange Consortium via the PRIDE [26] partner repository with the dataset identifier PXD013833.

Ingenuity Pathways Analysis software (IPA, QIAGEN) was used to classify genes onto canonical pathways, cellular and molecular functions and networks. Pathways enriched with a $P < 0.05$ were considered to be statistically significant. More details on IPA are found online (<http://www.ingenuity.com>). Database for Annotation, Visualization and Integrated Discovery (DAVID) software (<https://david.ncifcrf.gov>, Version 6.8) was used to determine and represent functional protein classes and biological processes enriched from Gene ontology (GO) database. Functional annotations with $P < 0.05$ (EASE score) (modified Fisher's exact test) were selected.

2.5. BrdU incorporation and cell cycle analysis

BrdU incorporation and DNA staining with PI were performed using the acid denaturation method as described previously [27]. All samples were analyzed by a FACSCanto flow cytometer (Becton Dickinson) and data were analyzed using Flowjo software.

2.6. Translation studies

After different treatments, cells were incubated in growth media containing 100 μg /cycloheximide for 15 min at 37 °C in order to stop ribosomal elongation. After being washed with ice-cold 1X PBS supplemented with 100 μg /ml cycloheximide, cells were scraped and harvested into ice-cold 1X PBS supplemented with 100 μg /ml cycloheximide and pelleted by centrifugation (3000 rpm for 5 min at 4 °C). The pellets were resuspended in 400 μl of LSB buffer (20 mM Tris-HCl pH 7.5, 100 mM NaCl, 3 mM $MgCl_2$, 1 mM DTT, 100 μg /ml of cycloheximide, and 100 U/ml of RNasin) and lysed by adding 400 μl of LSB buffer containing 2.4% Triton X-100 and 0.5 M sucrose. The lysates were centrifuged (12000 g for 5 min at 4 °C), and the supernatants were recovered and adjusted with additional 50 μl of LSB buffer containing NaCl and $MgCl_2$ with quantities that enable final concentrations of 50 mM NaCl and 7 mM $MgCl_2$. Then, supernatants were layered onto 15–50% sucrose gradients in LSB buffer, centrifuged (38,000 rpm for 2 h at 4 °C) and 18 fractions were collected with a fraction collector. For nonpolysomal RNA (fractions 1 to 8, containing ribosomal RNAs present in 40S, 60S, and 80S ribosomal complexes, and free mRNAs) and polysomal RNA (fractions 9 to 18, containing mRNAs bound to more than one ribosome), the optical density of these fractions (OD 254 nm) were determined.

2.7. Transcriptomic data analysis

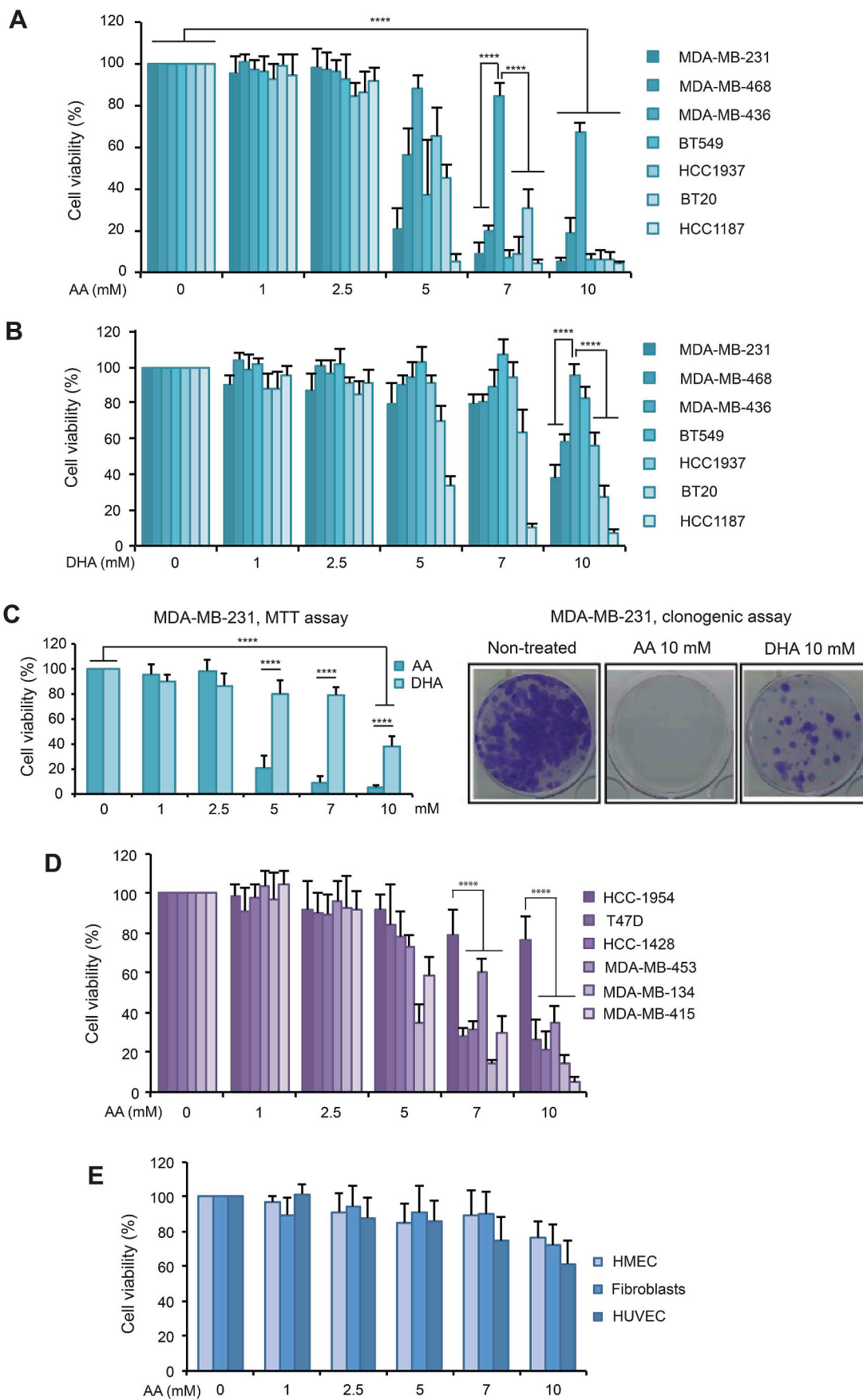
Genes expression data were extracted from two publicly accessible transcriptomic datasets: NCI-60 CellMiner Database (<https://discover.nci.nih.gov/cellminer/Database> Version: 2.1) and affymetrix normalized data for breast cancer cell lines of the Institut Curie collection (http://microarrays.curie.fr/publications/recherche_translacionnelle/plateforme_genomique/). Using NCI-60 CellMiner Database, each gene transcript Z-score (input HUGO name) and gene name were used as input identifier. The data file retrieved contained the average \log_2 intensity and Z-score of each gene expression in 60 cell lines. Using the Institut Curie database, gene mRNA expression levels (\log_2) for 29 breast cancer cell lines were retrieved.

2.8. Miscellaneous methods

MTT-based cell viability assay was performed as previously described [28]. For colony formation assays, cells were plated in 6-well plates in a density of 1000/well and treated under defined conditions and then further cultured for 14 days. Afterwards, colonies were fixed by ethanol, stained with crystal violet solution and counted using ImageJ software. For siRNA transfection, cells were transfected with 20 nM siRNA (ON-TARGET plus SMART pool siRNA or control siRNA, Dharmacon) using INTERFERin reagents (Polyplus Transfection). Further experiments were performed 48 h after transfection. Classical western blots and redox western blots were performed as described previously [24]. Total cellular glutathione levels (GSH + GSSG), GSSG (oxidized form) and GSH/GSSG ratios were assessed using GSH/GSSG-Glo™ Assay (Promega). Luminescence was read using TriStar² LB 942 Modular Monochromator Multimode Reader (Berthold technologies). Data were presented by GSH/GSSG ratios.

2.9. Statistical analysis

Statistical significance of each data set was analyzed using adequate



(caption on next page)

Fig. 1. Sensitivity of TNBC, non-TNBC and noncancerous cells toward AA and DHA. (A–B) Seven TNBC cell lines were treated with AA (A) or DHA (B) ranging from 0 to 10 mM for 24 h. Cell viability (%) relative to non-treated condition was measured with MTT assay for each cell line. Data are means ± SD of at least 6 independent experiments. Statistical significance is assessed by two-way ANOVA with Sidak's multiple comparisons test. (C) MDA-MB-231 cells were treated with AA or DHA for 24 h. Cell viability (%) relative to non-treated condition was measured by MTT assay (left panel). Data are means ± SD of at least 6 independent experiments. Representative images of colonies formation of MDA-MB-231 cells after AA or DHA treatments for 24 h are shown (right panel). (D) Six non-TNBC cells were treated with AA ranging from 0 to 10 mM for 24 h. Cell viability (%) relative to non-treated condition was measured with MTT assay. Data are means ± SD of at least 6 independent experiments. Statistical significance is assessed by two-way ANOVA with Sidak's multiple comparisons test. (E) HMEC, normal human dermal fibroblasts and HUVEC were treated with AA ranging from 0 to 10 mM for 24 h. Cell viability (%) relative to non-treated condition was measured with MTT assay for each cell line. Data are means ± SD of 4 independent experiments. Statistical significance is assessed by ordinary two-way ANOVA with Tukey's multiple comparisons test. ****, $P < 0.0001$.

statistical tests available in the GraphPad Prism 7 software and specified in the body of manuscript and figure legends. Data were presented as the mean ± standard deviation (SD). Dose-response modeling, half-maximal inhibitory concentration (IC50) determination from MTT cell viability assays and Spearman's correlation analyses were also performed using the GraphPad Prism 7 software (GraphPad Software, Inc). Wherever possible, exact P values are given and $P < 0.05$ were considered statistically significant.

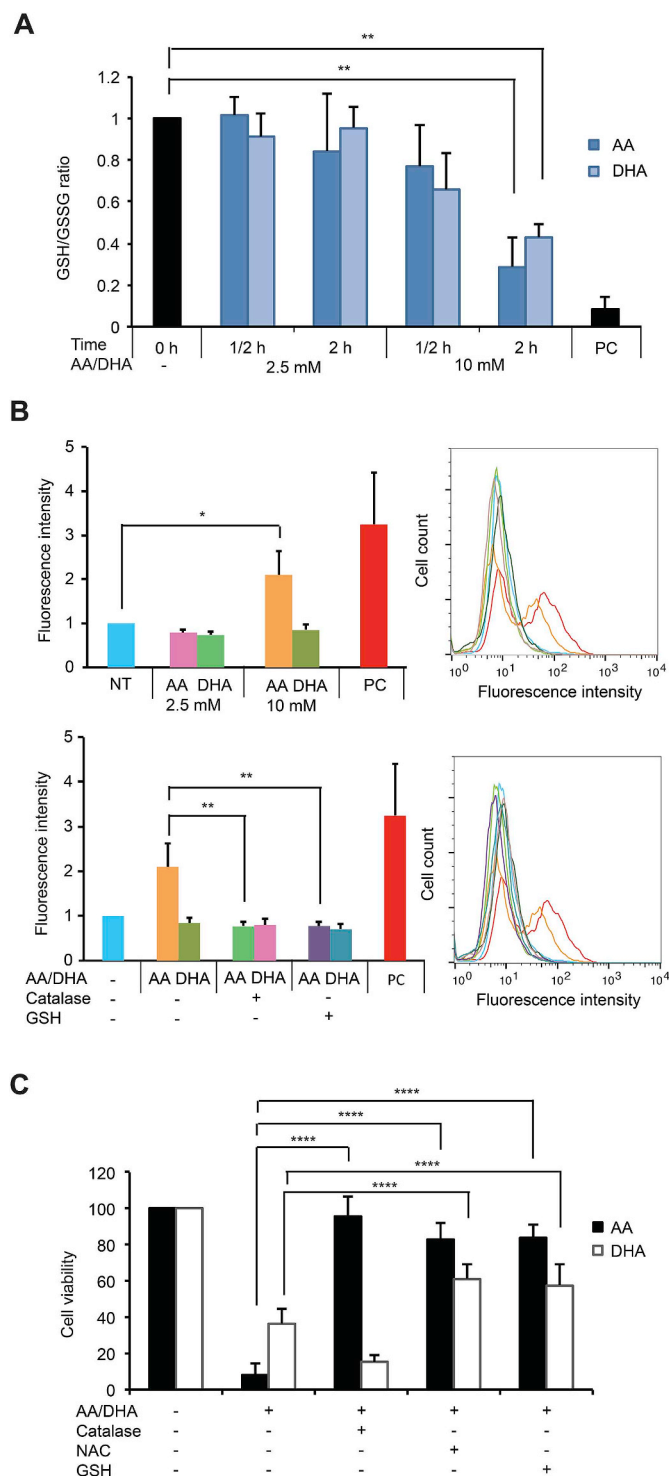
3. Results

3.1. AA shows higher cytotoxicity toward breast cancer cells than DHA without affecting noncancerous cells

A panel of 7 TNBC cell lines was exposed to increasing concentrations of AA and DHA. MTT assays showed that TNBC cells displayed different sensitivity to AA treatment for 24 h (Fig. 1A). At pharmacologic concentrations, MDA-MB-231 cells, among others (HCC-1187, BT549, MDA-MB-468, HCC-1937 and BT20), were highly sensitive to AA ranging from 7 mM to 10 mM (4–20% viability at 10 mM AA); while MDA-MB-436 showed more resistance (~70% viability at 10 mM AA). Less cytotoxicity was observed with DHA for all TNBC cells in the same treatment conditions. Only 3 cell lines (HCC-1187, BT20 and MDA-MB-231) were sensitive to 10 mM DHA treatment for 24 h (7–40% viability) (Fig. 1B). Upon AA and DHA treatments for 24 h, MTT assays and clonogenic assay confirmed that VitC-induced cytotoxicity was associated with a loss of the ability to form colonies and that AA displayed stronger cytotoxicity than DHA (Fig. 1C). In addition, we determined the sensitivity of 6 non-TNBC cell lines to AA-treatment for 24 h (Fig. 1D). Five of them (MDA-MB-134, T47D, HCC-1428, MDA-MB-415 and MDA-MB-453) were sensitive to 10 mM AA treatment (5–35% viability) while HCC-1954 showed more resistance (~80% viability). Finally, noncancerous cell lines including HMEC, human dermal fibroblasts and HUVEC showed a high survival rate even at 10 mM AA treatment (60–80%) (Fig. 1E).

3.2. H₂O₂ generation and GSH oxidation underlie AA-induced cytotoxicity while GSH oxidation plays a partial role in DHA-induced lower cytotoxicity

In order to understand the mechanism of action of AA and DHA, we used MDA-MB-231 cells, one representative TNBC cell line that is commonly studied in literature, to evaluate the redox alteration induced by VitC treatments. For this purpose, two concentrations of VitC were further used, the non-cytotoxic 2.5 mM and the cytotoxic 10 mM. Since DHA was shown to be responsible for GSH oxidation upon increased uptake through the glucose transporter GLUT1 in colorectal cancer model [10], we first determined the reduced and oxidized levels of this main cellular antioxidant after AA and DHA treatments in MDA-MB-231 cells. As shown in Fig. 2A, a significant decrease in GSH/GSSG ratios, indicating GSH oxidation, is observed after 2-h treatment with 10 mM AA or DHA but not with 2.5 mM. Next, we performed a general ROS assessment using carboxy-H₂DCFDA. A 2-fold increase in fluorescence intensity was detected upon treatment for 4 h with 10 mM but not with 2.5 mM AA (Fig. 2B). Co-treatment with 10 mM AA and either catalase or GSH abolished the increase in the fluorescence intensity



(caption on next page)

Fig. 2. Glutathione oxidation and ROS generation in response to AA and DHA treatments in MDA-MB-231 cells. (A) GSH and GSSG quantities were assessed in non-treated cells and cells treated with 2.5 or 10 mM AA or DHA for ½ hour and 2 h. Treatment with 250 µM diamide for 10 min was used as a positive control (PC). GSH/GSSG ratio value in non-treated cells is set as 1 and relative GSH/GSSG ratios calculated in treated conditions are represented as means ± SD of 4 independent experiments. Statistical significance is assessed by ordinary one-way ANOVA with Tukey's multiple comparisons test. (B) General intracellular ROS was assessed by flow cytometry using carboxy-H₂DCFDA probes in non-treated cells (NT), cells treated with 2.5 or 10 mM AA or DHA for 4 h (upper panel), cells treated with 10 mM AA, 10 mM AA plus 2000 U/ml catalase or 10 mM AA plus 10 mM GSH (lower panel). Treatment with 100 µM H₂O₂ for 20 min was used as a positive control (PC). Mean fluorescence value in non-treated MDA-MB-231 cells is set as 1 and relative fluorescence intensity is represented. Data are means ± SD of 4 independent experiments. Statistical significance is assessed by ordinary one-way ANOVA with Tukey's multiple comparisons test. (C) MTT assay was performed on cells treated with 10 mM AA or DHA alone or in the presence of 2000 U/ml catalase, 10 mM NAC or 10 mM GSH for 24 h. Data are means ± SD of at least 6 independent experiments. Statistical significance is assessed by two-way ANOVA with Tukey's multiple comparisons test. ****, $P < 0.0001$; **, $P < 0.01$; *, $P < 0.05$.

observed. In contrast, 10 mM DHA did not result in change in fluorescence intensity that was not affected either by the presence of catalase or GSH (Fig. 2B). This indicates that cytotoxic dose of AA treatment, but not DHA, induces general intracellular ROS accumulation.

We then questioned the link between these redox alterations and VitC cytotoxicity. Noticeably, AA-induced cytotoxicity in MDA-MB-231 cells could be totally or largely suppressed by the presence of either catalase, NAC or GSH (Fig. 2C). NAC serves as a prodrug to L-cysteine which is a precursor to GSH. On the other hand, DHA-induced cell death was not rescued by catalase, while partially by GSH or NAC, with mean cell viability 58% and 61% respectively. These observations indicate the role of H₂O₂ generation and GSH oxidation in AA cytotoxicity and a partial implication of GSH oxidation in DHA cytotoxicity.

To further verify the generation of H₂O₂ in AA-treated condition, we used Amplex-Red Kit to measure H₂O₂ concentration in the medium. After 10 mM AA treatment for 5 min, ½ hour and 2 h, H₂O₂ concentrations in the medium with or without MDA-MB-231 cells increased more than 20 times (Fig. 3A). Furthermore, the co-treatment by AA and catalase abolished H₂O₂ accumulation, validating the extracellular generation of H₂O₂ by AA. Next, we used genetically encoded HyPer sensors addressed to several cellular compartments in MDA-MB-231 cells to determine whether H₂O₂ accumulated intracellularly in one or more cellular compartments. HyPer sensors specifically react with H₂O₂ [29,30]. Cytoplasm-localized HyPer oxidation was visible in presence of 10 mM AA for 5 min, ½ hour and 2 h, indicating a continuous H₂O₂ accumulation in the cytoplasm of the cells upon AA treatment (Fig. 3B). The same results were obtained with nucleus-, mitochondrial matrix- and membrane-targeted HyPer. Furthermore, co-treatment with AA and catalase abolished the oxidation of HyPer. Finally, the redox states of two compartment-specific antioxidant proteins, cytoplasmic PRDX1 and mitochondrial PRDX3, were analyzed by redox Western blot. Cytotoxic dose of AA (10 mM) increased PRDX3 oxidation (50–60% dimer) and PRDX1 oxidation (~10% dimer) after 5 min, ½ hour and 2 h of treatment, indicating mitochondrial and cytosolic H₂O₂ accumulation (Fig. 3C). These data are in agreement with an important role of H₂O₂ in AA-induced cytotoxicity.

3.3. AA treatment alters the redox state of cysteine-containing proteins

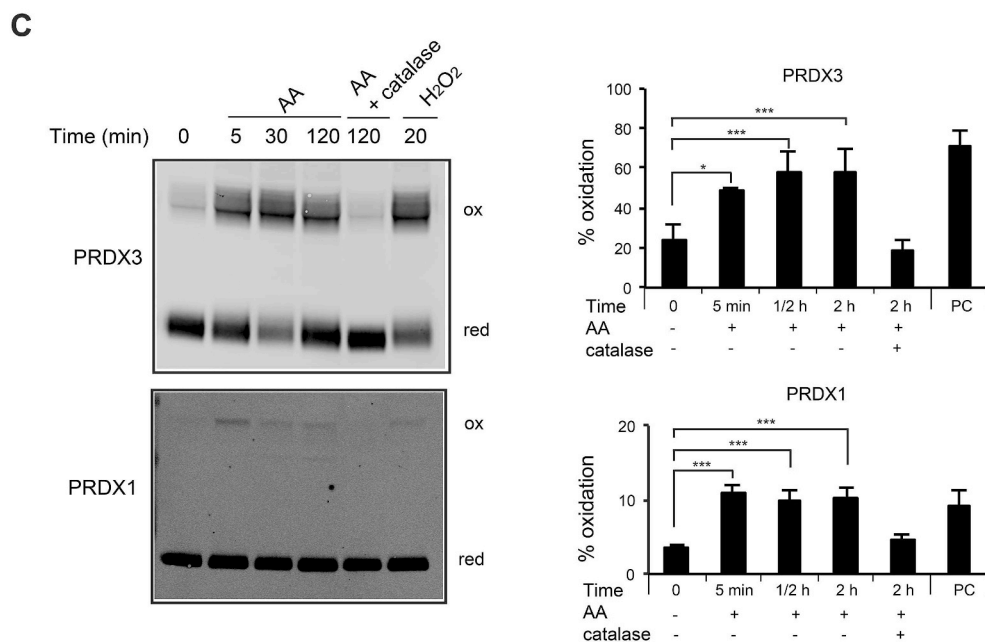
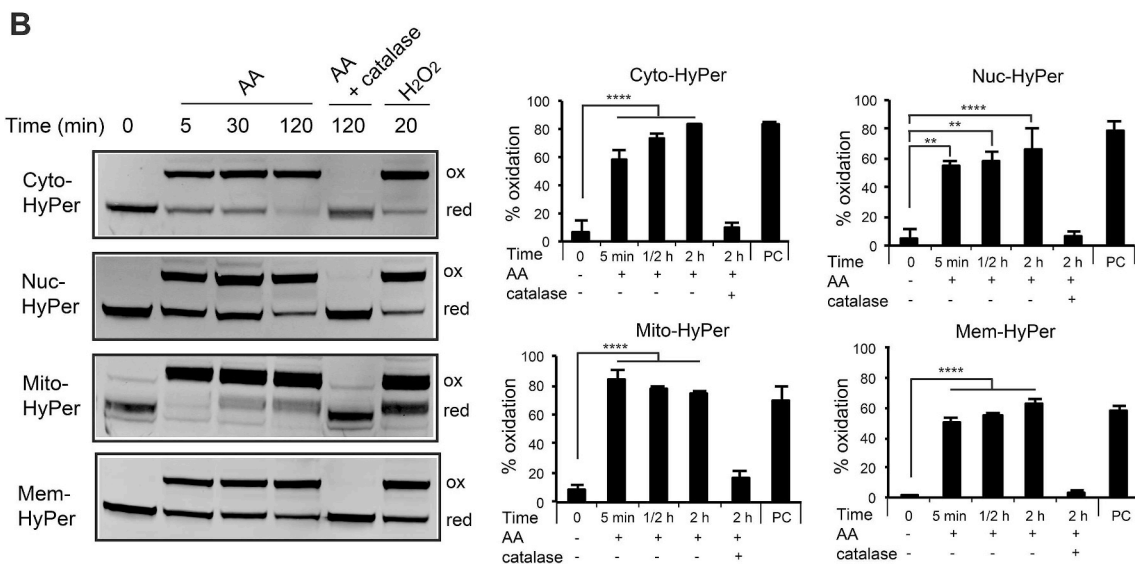
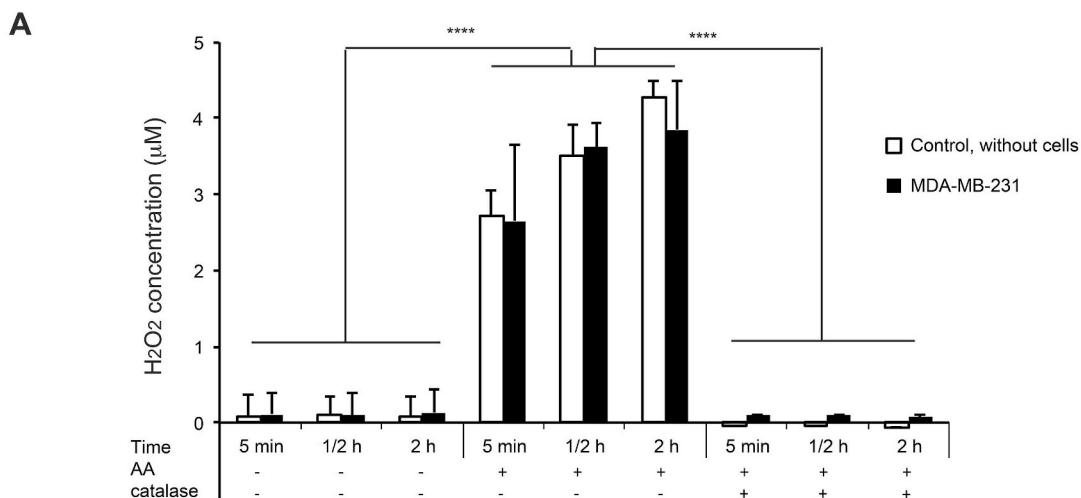
Our observations described above linked AA cytotoxicity to extracellular and intracellular H₂O₂ accumulation and showed the redox state alteration of some cysteine-containing antioxidants upon AA treatment. As many proteins with highly reactive cysteine residues are implicated in different critical pathways and could be impacted by

H₂O₂, we decided to examine the alterations of the redoxome, the oxidized proteome of cysteine-containing proteins, by redox mass spectrometry approach [31,32]. Using a biotin switch approach that allows the enrichment of proteins containing oxidized thiols [25], we compared the redoxome of non-treated and treated (10 mM AA, ½ hour) MDA-MB-231 cells in two independent biological replicates, each with three technical replicates (Supplementary Fig. 1). Upon short AA treatment, we expected to identify early events in cellular response to AA that might be linked to AA-induced cell death.

Quantitative proteomic analysis by LC-MS/MS allowed the identification of 2910 cysteine-containing proteins. Among them, 203 proteins (6.97%) were commonly identified in both biological experiments and exhibited a significant change in cysteine oxidation levels between non-treated and treated cells (over 1.5-fold in at least one of the two biological experiments with $P < 0.05$) (Supplementary Table 1). 38.42% of these proteins were more oxidized while 61.58% were more reduced in 10 mM AA-treated cells compared to the non-treated condition. The high proportion of more reduced proteins following AA treatment is intriguing but could be explained by the fact that intracellularly AA could not only generate H₂O₂ but also act as a conventional reducing agent, generating both oxidized and reduced proteins upon AA treatment. Compartment-specific redox response could also be taken into account. Proteins in some compartments could be more oxidized while those in other compartments could be more reduced through antioxidant system response against the AA-induced H₂O₂ and oxidative stress, thus protecting some important cellular signaling pathways and proteins from oxidation.

As expected, antioxidant enzymes including glutathione S-transferase Mu 3 (GSTM3), γ -glutamylcyclotransferase (GGCT) and PRDX1 were among the identified oxidized targets of AA treatment (Supplementary Table 1), compromising antioxidant capacity. On the other hand, proteins belonging to the glycolysis and gluconeogenesis pathway (PYGM, PGK1), and tricarboxylic acid cycle (ACOT7, DLAT, FADS2), exhibited also a significant increase in oxidation upon AA treatment. Thus, energetic metabolism enzymes were also among the targets of AA, in accordance with the energetic crisis and metabolic alterations described in other studies [33]. Interestingly, several proteins implicated in DNA and RNA metabolism as well as in protein metabolism were oxidized in treated cells, including chromosome-associated kinesin KIF4A (accession number O95239), histone-binding protein RBBP4 (Q09028), ATP-dependent RNA helicase DHX8 (Q14562), U5 small nuclear ribonucleoprotein 40-kDa protein (Q96DI7), tRNA-splicing ligase RtcB homolog (Q9Y310), 26S proteasome non-ATPase regulatory subunit 3 (O43242), Cullin-4A (Q13619), E3 ubiquitin-protein ligase RING2 (Q99496), E3 ubiquitin-protein ligase UBR4 (Q5T4S7), E3 ubiquitin-protein ligase XIAP (P98170), and E3 SUMO-protein ligase RanBP2 (P49792) (Supplementary Table 1). These data indicate that AA leads to the oxidation of thiol-containing proteins implicated in several essential cellular processes such as energy production, nucleic acid and protein metabolisms.

IPA software for enrichment analysis of these 203 proteins differentially oxidized between AA-treated and non-treated conditions revealed that glucocorticoid receptor signaling and EIF2 signaling pathways were among the top significant canonical pathways (Fig. 4A). The top five significantly enriched molecular and cellular pathways included cellular assembly and organization, cellular function and maintenance, RNA post-transcriptional modification, molecular transport and RNA trafficking (Fig. 4A). These proteins' main networks were dominated by RNA post-transcriptional modification, cancer, cell death and survival (Fig. 4A). Moreover, protein classification according to their GO biological processes in DAVID database fall into categories of cell-cell adhesion, rRNA processing, translational initiation, viral transcription, and cell proliferation, among others (Fig. 4B). Taken together, redoxome data seem to point to the possible effect of AA treatment on DNA replication and transcription/translation, among other pathways.



(caption on next page)

Fig. 3. Extracellular and intracellular H₂O₂ accumulation upon AA treatment in MDA-MB-231 cells. (A) Using Amplex-Red Kit, H₂O₂ concentration was measured in the medium in the presence of MDA-MB-231 cells, without treatment or treated with 10 mM AA alone, 10 mM AA plus 2000 U/ml catalase, for 5 min, ½ hour and 2 h. The same measurements were done on the medium without cells as controls. Quantifications are means ± SD of 3 independent experiments. (B) Cells transiently expressing respectively cytoplasm-, nucleus-, mitochondria- and cell membrane-targeted HyPer were not treated or treated with 10 mM AA alone or together with 2000 U/ml catalase for 5 min, ½ hour and 2 h. Treatment with 100 μM H₂O₂ for 20 min was used as a positive control (PC). HyPer redox state was evaluated by redox Western blot. ox, oxidized form; red, reduced form. Graphs show the quantification of oxidized HyPer (%) vs total HyPer protein. Quantifications are means ± SD of 3 independent experiments. (C) Redox state of PRDX1 and PRDX3 was assessed using redox Western blot in cells without treatment or treated with 10 mM AA alone, 10 mM AA plus 2000 U/ml catalase, for 5 min, ½ hour and 2 h. Treatment with 100 μM H₂O₂ for 20 min was used as a positive control (PC). ox, oxidized form; red, reduced form. Quantifications of oxidized PRDX1 or PRDX3 (%) vs total protein in MDA-MB-231 cells are means ± SD of 3 independent experiments. Statistical significance is assessed by ordinary one-way ANOVA with Tukey's multiple comparisons test. ****, $P < 0.0001$; ***, $P < 0.001$; **, $P < 0.01$; *, $P < 0.05$.

3.4. S-phase of cell cycle is affected by AA treatment

As a first attempt, we performed cell cycle analysis on MDA-MB-231 cells upon AA treatment using BrdU. BrdU is a thymidine analogue which can be incorporated into the DNA during replication. BrdU staining thus allows to follow newly synthesized DNA together with total DNA staining by PI to measure total DNA content and assign the cells to the various stages of the cell cycle. Cells were left non-treated or treated with 10 mM AA for 2 h. Then, at various time points of post-treatment recovery (from 0 to 24 h), cells were pulse-labeled with BrdU followed by PI staining and FACS analysis. A significant decrease in BrdU incorporation was observed after 2 h of AA treatment, indicating an S-phase arrest when compared to non-treated cells (Fig. 5A and B). To support these data, cells were first labeled with BrdU, and then treated or not with 10 mM AA for 2 h before being analyzed by FACS at various time points during post-treatment recovery. Cells subjected to AA treatment showed an immediate and prolonged S-phase delay (Fig. 5C). Moreover, catalase efficiently prevented S-phase slowdown in both conditions of BrdU pulse, post and prior AA treatment (Fig. 5A–C), suggesting that H₂O₂ production is causal in the inhibition of DNA replication. Taken together, these observations point to the possibility that the inhibition of DNA replication is one of the causes of AA cytotoxicity.

3.5. Translation inhibition in response to AA treatment

We next performed polysome profiling to monitor translation activity of mRNA in MDA-MB-231 cells upon AA treatment. Cellular RNAs were extracted and fractionated in a 15–50% sucrose gradient. When comparing nonpolysomal RNA and polysomal RNA quantities between non-treated cells and cells treated with 10 mM AA for 2 h, a significant decrease in polysomal RNA ($62 \pm 5\%$ vs $44 \pm 2\%$) accompanied with a significant increase in nonpolysomal RNA ($38 \pm 5\%$ vs $56 \pm 2\%$) occurred, reflecting a decrease of cellular translation activity upon AA treatment (Fig. 6A and B). Moreover, adding catalase (2000 U/ml) that rescued cell viability rescued partially the cellular translation activity as seen for polysomal RNA ($44 \pm 2\%$ in AA-treated cells vs $53 \pm 6\%$ in AA plus catalase-treated cells) and for nonpolysomal RNA ($38 \pm 5\%$ vs $47 \pm 6\%$) (Fig. 6A and B). Taken together, these data suggest that the AA-induced inhibitory effect on mRNA translation contributes to AA cytotoxicity.

3.6. H₂O₂ scavenging system including PRDX1 is linked to variable cellular sensitivity to AA

The different sensitivity to AA among TNBC and non-TNBC cells prompted us to identify gene and protein expressions that correlate with AA anticancer activity. Pattern comparison using the NCI-60 CellMiner web tool [34,35] was performed to assess the correlation between gene expression and AA cytotoxicity. Significant negative Pearson's correlations (meaning that the more a gene is expressed, the more cells are resistant to AA) were defined at $r < -0.334$ based on a minimum of 35 informative cell lines, and P value < 0.05 in the absence of multiple comparisons. This analysis allowed us to identify 246

genes with transcript levels correlated negatively and significantly with AA cytotoxicity (Supplementary Table 2). *PTGRI* had the highest significant correlation value ($r = -0.608$, $P = 0$) and was already highlighted in our earlier work as a predictive biomarker for resistance of breast cancer cell lines to auranofin/VitC combinational cytotoxicity [28]. For AA alone, expressions of some antioxidant genes such as *TXNRD1* ($r = -0.401$, $P = 1.624 \times 10^{-3}$) and *PRDX1* ($r = -0.384$, $P = 2.678 \times 10^{-3}$) also correlated negatively with AA cytotoxicity.

We performed a pathway analysis using the IPA software for the 246 genes. NRF2-mediated oxidative stress response was the first significant canonical pathway enriched (Supplementary Fig. 2A). Top statistically significant molecular and cellular pathways for these genes included cellular movement and cell death and survival, among others. Finally, the top networks of these genes included cancer, cell death and survival and carbohydrate metabolism. Protein classification according to their GO biological processes in DAVID database highlighted a significant association with signal transduction, oxidation-reduction process, and response to oxidative stress, among others (Supplementary Fig. 2B). All these data directed us to conclude that oxidative stress response genes play a role in the resistance of cancer cells to H₂O₂-mediated cytotoxicity of AA.

We wanted to ascertain that, for these genes, the predicted negative correlation of their expression with AA activity according to NCI-60 database are indeed valid on breast cancer cell lines. We thus calculated IC₅₀ of AA on 13 breast cancer cell lines (Supplementary Fig. 3) and correlated them with the retrieved gene expression data from the Institut Curie database. Fig. 7A shows *PRDX1* gene expression (mRNA) distribution of 29 breast cancer cell lines. A correlation between AA activity (log₁₀IC₅₀) and *PRDX1* expression levels (log₂) was statistically significant and valid for most of the breast cancer cell lines studied (Spearman's correlation $r = 0.5769$, $P = 0.0425$) (Fig. 7B and C). By knocking down *PRDX1* gene, the highly resistant HCC-1954 became significantly more sensitive to 10 mM AA, MDA-MB-436 cells became significantly more sensitive to 5 or 10 mM AA (Fig. 7D and E), and MDA-MB-231 cells became significantly more sensitive to 2.5 mM AA (Fig. 7F). Consistently, we previously showed that *PRDX1* knockdown sensitizes HeLa and A549 cancer cells toward ROS-generating anticancer molecules [24,36]. More recently, other researchers reported inhibitory effect of *PRDX1*-knockout on growth of mammary tumor in mouse model, enhancing VitC cytotoxicity [37]. Finally, NCI-60 data also indicate that lung cancer cells that are mostly resistant to AA have high *PRDX1* expression (Supplementary Fig. 4). Further experiments on larger panel of cells in each cancer type are needed for achieve firm conclusions on the predictive value of *PRDX1* expression.

4. Discussion

Anticancer effect of VitC at pharmacologic concentrations has been largely attributed to H₂O₂ extracellular generation from AA [4,6–8,38,39]. However, one study reported that VitC selectively kills KRAS and BRAF mutant colorectal cancer cells by targeting GAPDH via DHA [10]. Here we showed that AA displayed much higher cytotoxicity than DHA in 13 breast cancer cell lines. Normal cells including HMEC, human dermal fibroblasts and HUVEC were much less affected by AA

A

Top Canonical Pathways			
Name	P value	Overlap	
Glucocorticoid Receptor Signaling	2.75E-11	5.8 %	20/345
EIF2 Signaling	1.55E-09	6.6 %	15/227
Integrin Signaling	2.38E-05	4.6 %	10/219
Germ Cell-Sertoli Cell Junction Signaling	2.88E-05	5.0 %	9/179
Lipid Antigen Presentation by CD1	7.24E-05	15.4 %	4/26

Molecular and Cellular Functions		
Name	P value	# Molecules
Cellular Assembly and Organization	8.73E-03 – 1.42E-09	67
Cellular Function and Maintenance	8.73E-03 – 1.42E-09	68
RNA Post-Transcriptional Modification	1.27E-03 – 1.64E-09	20
Molecular Transport	7.39E-03 – 2.15E-08	37
RNA Trafficking	4.02E-04 – 2.15E-08	8

Top Networks	
ID Associated Network Functions	Score
1. RNA Post-Transcriptional Modification, Cancer, Cell Death and Survival	68
2. Dermatological Disease and Conditions, Developmental Disorder, Organismal Injury and Abnormalities	50
3. Embryonic Development, Organismal Development and Tissue Development	45
4. Cell Morphology, Cellular Assembly and Organization, Cardiovascular Disease	40
5. Gene Expression, Cancer, Gastrointestinal Disease	33

B

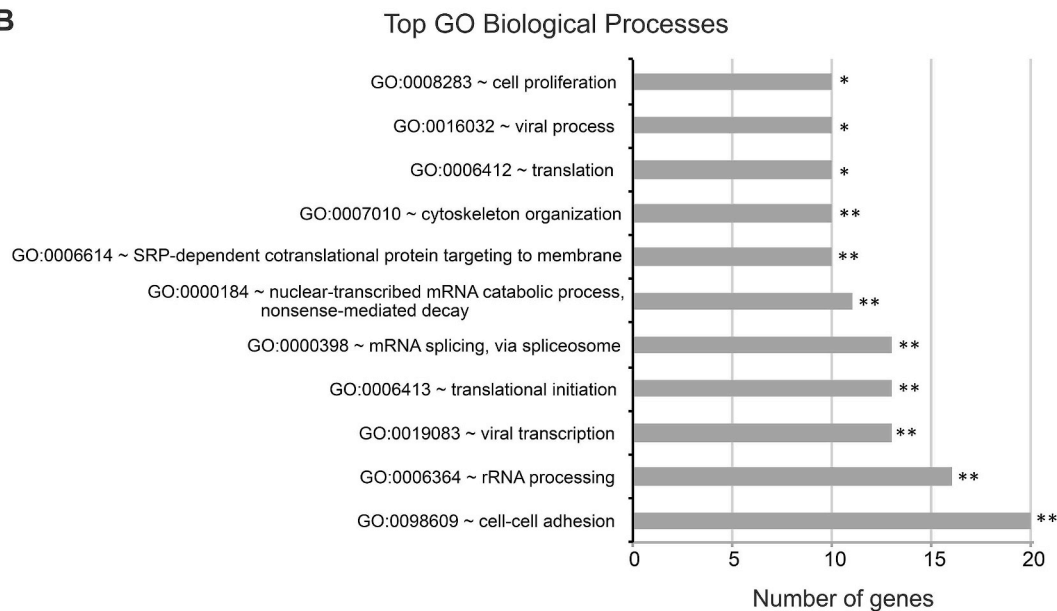
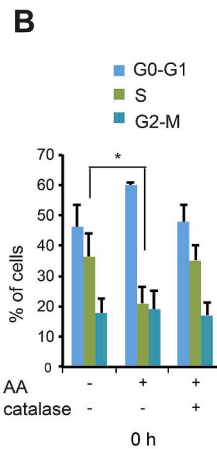
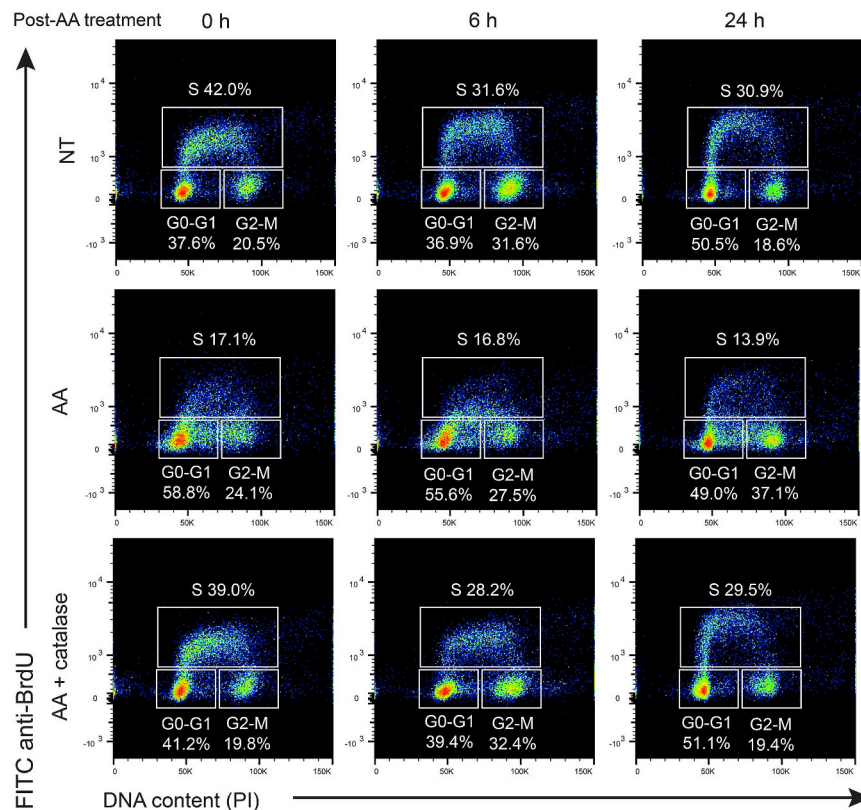
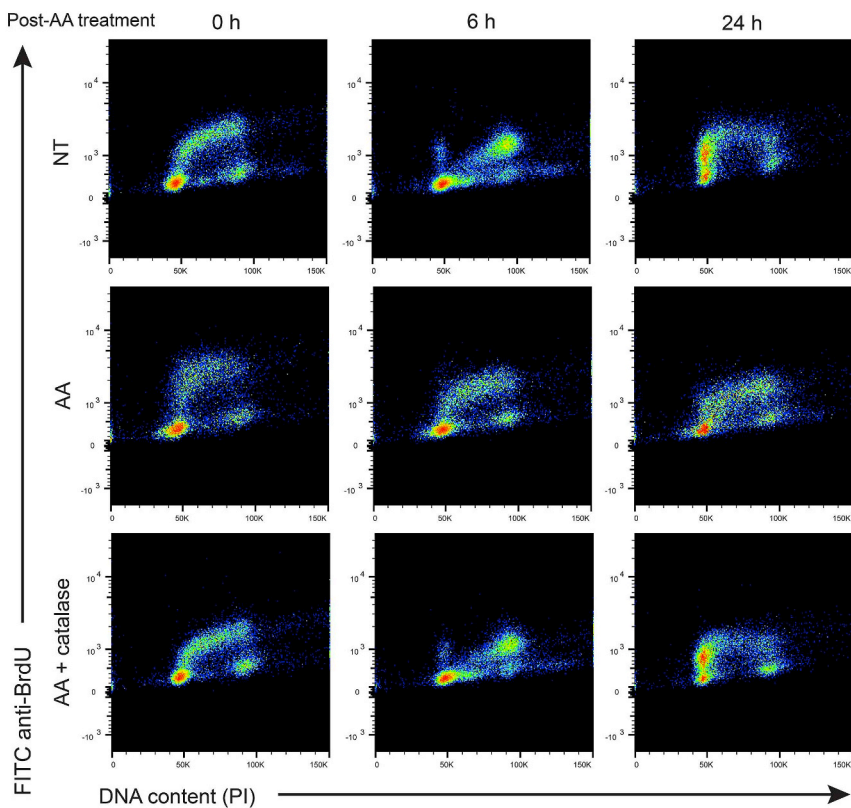


Fig. 4. Pathway, function and network analysis of the differentially oxidized cysteine-containing proteins identified by “redoxome” upon AA treatment. The alterations of the oxidized proteome of cysteine-containing proteins, after 10 mM AA treatment for ½ hour in MDA-MB-231 cells were analyzed by mass spectrometry. 203 differentially oxidized proteins with $P < 0.05$ and a fold change over 1.5 in at least one of the two biological experiments were identified between AA-treated and non-treated cells. (A) Significantly altered cysteine-containing proteins were mapped by the IPA analysis software. The top 5 significantly associated canonical pathways, molecular and cellular functions and networks of these proteins are represented. (B) Altered proteins were classified according to their GO biological process pathways in DAVID database. The top significantly (Fisher's modified test) associated biological processes are represented. **, $P < 0.01$; *, $P < 0.05$.

A +/- AA treatment → Recovery → BrdU for 1 h → PI staining → FACS



C BrdU for 1 h → +/- AA treatment → Recovery → PI staining → FACS



(caption on next page)

Fig. 5. Effect AA treatment on cell cycles of MDA-MB-231 cells. (A) Non-treated (NT) cells, cells treated for 2 h with 10 mM AA, 10 mM AA plus 2000 U/ml catalase were released in fresh medium. At various time points of post-treatment recovery (from 0 to 24 h), these cells were stained with BrdU for 1 h followed by PI staining and FACS analysis. Dot plots of samples from 0, 6 and 24 h post-treatment recovery are presented with values of the percentages (%) of the population in each phase of cell cycle (G0-G1, S, G2-M). (B) Histogram shows the percentages (%) of cells in G0-G1, S, G2-M phases at 0 h post-AA treatment as means \pm SD calculated from 3 independent experiments. Statistical significance is assessed by one-way ANOVA with Tukey's multiple comparisons test. *, $P < 0.05$. (C) MDA-MB-231 cells were labeled with BrdU for 1 h and then subjected to three treatment conditions for 2 h: non-treatment (NT), treated with 10 mM AA, or 10 mM AA plus 2000 U/ml catalase. Cells were then analyzed by flow cytometry after PI staining at different time points during recovery in growth media (0, 6 or 24 h). Representative graphs of at least 3 experiments are shown.

treatment. While most of breast cancer cell lines were sensitive to AA similar to MDA-MB-231 cells, some cell lines, such as HCC-1954 and MDA-MB-436, were more resistant. AA-induced cytotoxicity toward MDA-MB-231 cells was entirely linked to extracellular H₂O₂ generation and intracellular accumulation in different compartments together with GSH oxidation.

Since H₂O₂ is the main player in AA cytotoxicity, we analyzed redoxome in MDA-MB-231 cells in order to reveal a general oxidation

spectrum of cysteine-containing proteins in response to AA. The short-time AA treatment (½ hour) unlikely affects basal protein abundance and therefore is less likely to bias protein oxidation data. Indeed, Western blot for several randomly selected individual proteins that showed a significant change in oxidation/reduction state of cysteines following AA treatments indicated no change in total protein abundance under the same condition as used in redoxome study (data not shown). As expected, AA oxidizes antioxidant proteins such as PRDX1

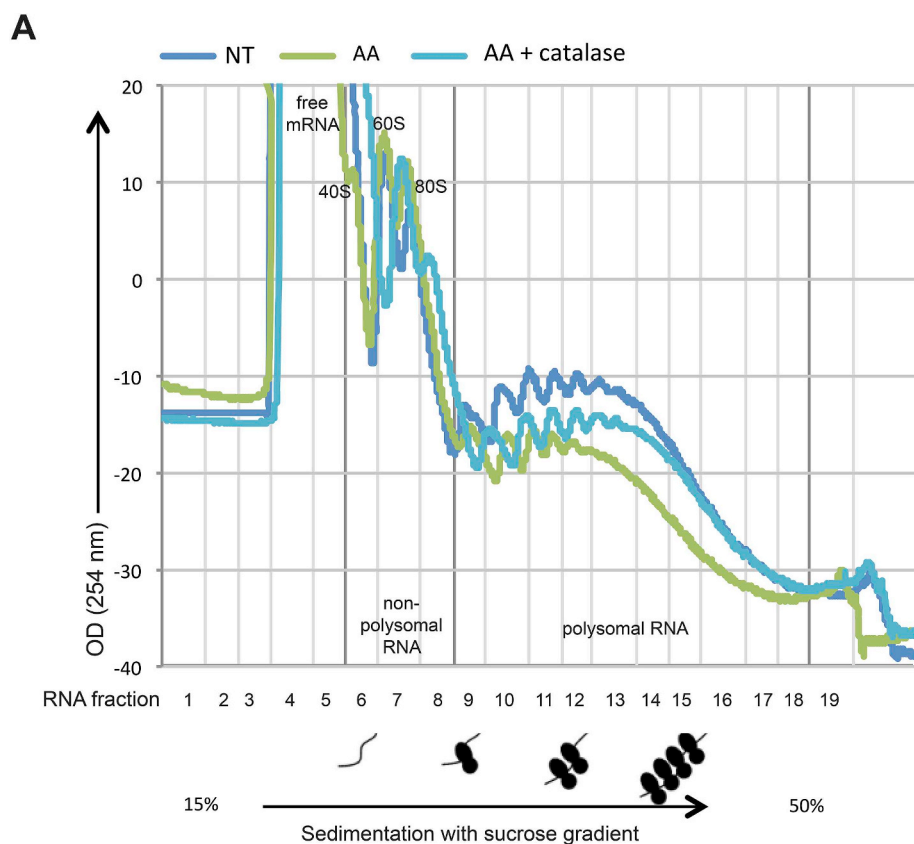
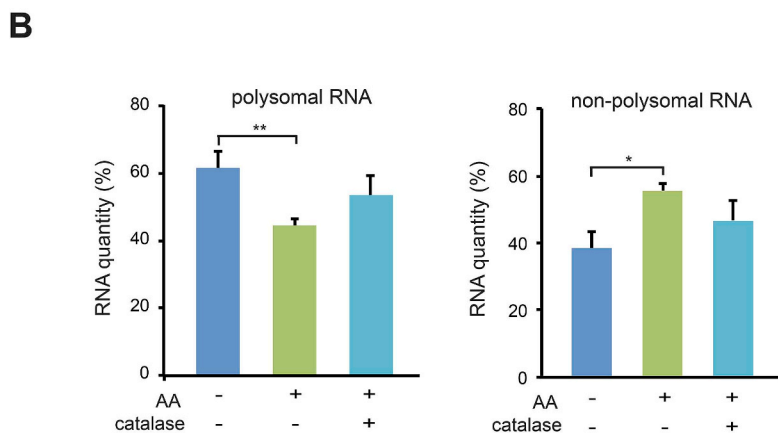


Fig. 6. Effect AA treatment on polysome gradient profiles of MDA-MB-231 cells. (A) Non-treated (NT) cells, cells treated for 2 h with 10 mM AA, 10 mM AA plus 2000 U/ml catalase were incubated for 15 min with cycloheximide to stop ribosomal elongation. Cellular RNA was extracted and fractionated in a 15–50% sucrose gradient. Optical density profiles (OD 254 nm) of polysome gradient profiles are shown, and non-polysomal RNA corresponding to fractions 1 to 8 (containing ribosomal RNAs present in 40S, 60S, and 80S ribosomal complexes and free mRNAs) and polysomal RNA corresponding to fractions 9 to 18 (containing mRNAs bound to more than one ribosome) are indicated. (B) The areas under the curve (AUC) of the optical density profiles of non-polysomal and polysomal RNA were measured, the percentage of non-polysomal or polysomal RNA relative to total was then calculated. Quantifications are represented in graphs as means \pm SD of 3 independent experiments. Statistical significance is assessed by ordinary one-way ANOVA with Tukey's multiple comparisons test. **, $P < 0.01$; *, $P < 0.05$.



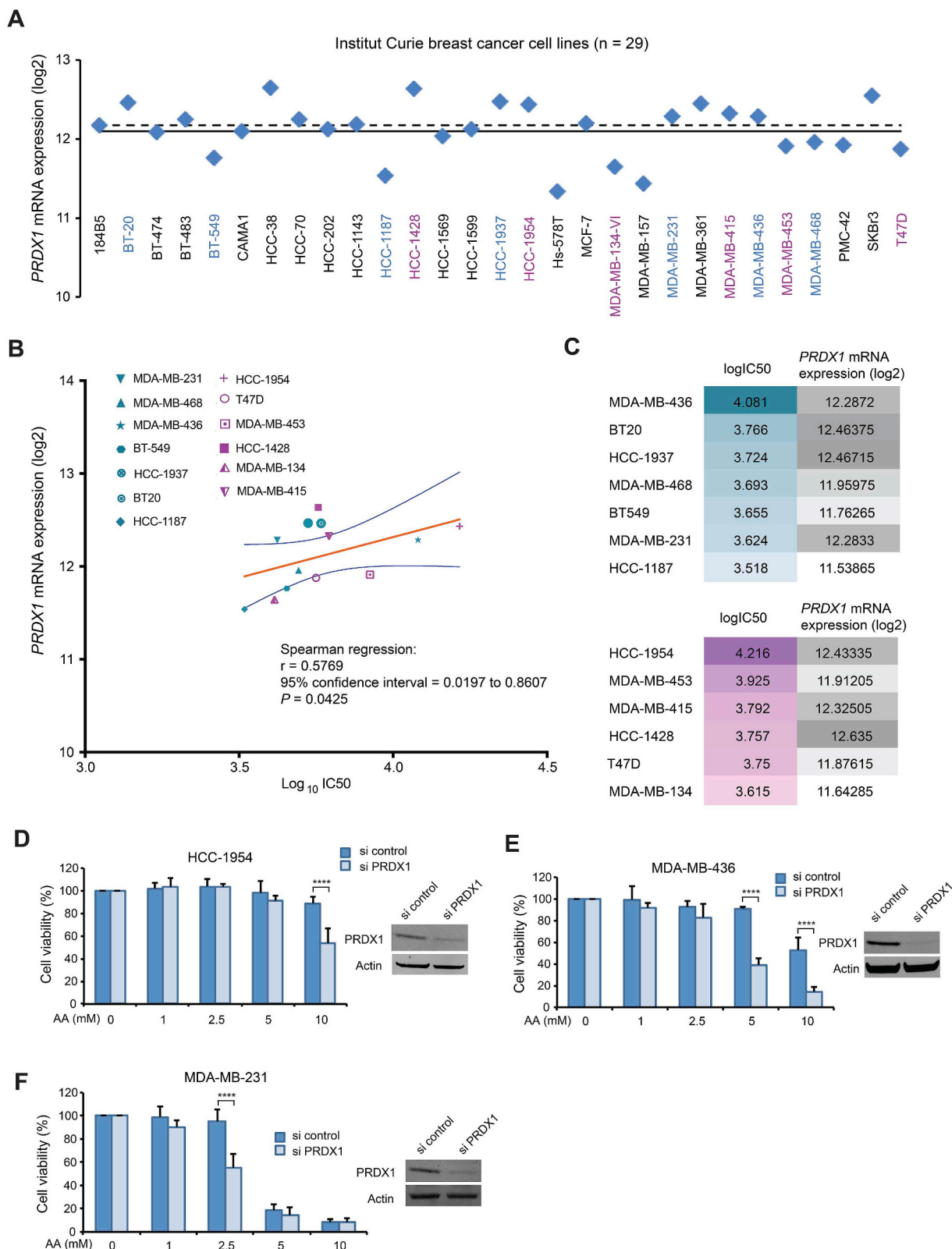


Fig. 7. PRDX1 expression and its link to breast cancer cellular response to AA. (A) PRDX1 mRNA expression patterns in log₂ values in 29 breast cancer cells retrieved from publicly available transcriptomic datasets of the Institut Curie breast cancer cell lines. Mean and median values are shown as solid and dashed lines, respectively. (B) Spearman's correlation analysis corresponding to PRDX1 mRNA expression vs IC50 for AA on 13 breast cancer cell lines. IC50 values were calculated from MTT assays for cell viability. Spearman's correlation was performed using GraphPad software. The 7 TNBC cell lines are indicated by green symbols and the 6 non-TNBC cell lines by purple symbols. The best-fit line is in solid orange line and the 95% confidence bands of the best-fit line are indicated in blue lines. Mathematical parameters are represented next to the graphs. (C) logIC50 of AA for breast cancer cell lines and their PRDX1 mRNA expression in log₂ values. (D-E-F) MTT assay on HCC-1954, MDA-MB-436 and MDA-MB231 cells transiently transfected with PRDX1 specific siRNA or control siRNA for 48 h followed by treatments with different concentrations of AA for 24 h. The insert is Western blot to verify efficiency of PRDX1 knockdown in siRNA transfected cells. Statistical significance is assessed by two-way ANOVA with Sidak's multiple comparisons test. ****, $P < 0.0001$.

and GGCT, very probably affecting the thioredoxin and glutathione scavenging systems. Furthermore, AA alters the redox state of many proteins implicated in the metabolic process, providing a rational explanation for a set of previously reported data that AA induced metabolic alterations, impairing glycolysis [10], pentose phosphate pathway, glycolysis and tricarboxylic acid cycle [18], impairing the Warburg metabolism and downregulating glucose transporters and pyruvate kinase M2 in cancer cells [33].

Several proteins involved in RNA metabolism and related pathways such as rRNA processing and translational initiation were significantly enriched in redoxome data upon AA treatment. Consistently, we showed a strong inhibitory effect of AA on mRNA translation in MDA-MB-231 cells, indicating that mRNA translation inhibition is one of the possible mechanisms responsible for oxidative stress-based AA cytotoxicity. This is in accordance with the fact that cells globally downregulate translation as quick adaptive response to stress [40]. In fact, cells resort to translational reprogramming toward selective translation of mRNAs encoding vital proteins, involved in survival and stress recovery, in an attempt to alleviate cellular burden under unfavorable conditions [41]. It is worth noting that since recognizing the important role played by deregulated translation in carcinogenesis [42], the repression or blockage of protein synthesis has gained a significant interest as a promising anticancer strategy [43,44]. Similarly, a set of proteins implicated in DNA metabolism and related cell proliferation pathway were found among the proteins with oxidized cysteine upon AA treatment. Indeed, cell cycle of MDA-MB-231 cells was impaired upon AA treatment for 2 h, suggesting potential involvement of DNA replication inhibition in AA cytotoxicity. It is shown that AA, via H_2O_2 generation, induces time- and concentration-dependent genotoxic stress and DNA damage and activates the ataxia telangiectasia mutated (ATM)/adenosine monophosphate-activated protein kinase (AMPK) pathway, all of which inhibit the mammalian target of rapamycin (mTOR) signaling pathway connected to cell proliferation, inducing cell death in ovarian cancer cells [19]. On the other hand, a direct impact of VitC and vitamin K3 combination on ribonucleotide reductase (RNR) was observed [45]. RNR activity was directly inhibited by the H_2O_2 generated along with the limited electron supply upon thioredoxin and glutathione oxidation by the combination of the two molecules. RNR is essential for *de novo* production of deoxyribonucleotides that is highly needed in cancer cells, thus RNR could be the link between VitC, DNA replication impairment and cancer cell death [45].

The mechanism by which VitC kills cancer cells while sparing normal cells is not entirely clear. It could be linked to a differential ability to metabolize H_2O_2 between normal and cancer cells [11], differential SVCT2 expression [14], or to cancer cells altered redox-active iron metabolism [15]. Our redoxome data and bioinformatics analysis indicate that AA-generated H_2O_2 can target multiple pathways at the same time, which might be particularly deleterious for cancer cells that strongly rely on antioxidants and metabolic reprogramming for survival, contributing cytotoxic selectivity of AA in cancer vs normal cells.

Our bioinformatics analysis also revealed that proteins belonging to the antioxidant system or NRF2-mediated oxidative stress response are linked to variable cellular sensitivity to AA (Supplementary Fig. 2A). Precisely, *PRDX1* gene expression correlated significantly with the response of breast cancer cell lines to AA, as cells with higher *PRDX1* expression were more resistant to AA, and *PRDX1* knockdown enhanced cellular sensitivity to AA. *PRDX1* is a key antioxidant that is directly involved in H_2O_2 elimination, thus has a protective activity against AA-generated H_2O_2 and could indeed be linked to AA resistance. *PRDX1* prediction value to AA treatment outcome warrants further validation in pre-clinical and clinical studies.

In summary, combined with previously reported data in the literature, this work provides insights on differential breast cancer cell line response toward AA and DHA treatments (Fig. 8). We first showed an extracellular generation of H_2O_2 by AA, but also an intracellular accumulation of H_2O_2 . Intracellular H_2O_2 can be transported from the

extracellular medium by aquaporins or by passive diffusion across plasma cellular membranes [46] but also generated by intracellular AA upon import through SVCTs (mainly SVCT2) [47]. Although in breast cancer cells, AA may not be imported by SVCT2, but only to mitochondria via mitochondrial SVCT2 (mitSVCT2), AA can be oxidized extracellularly to DHA and then imported through glucose transporters to be reduced by GSH-dependent mechanisms to AA intracellularly [48], consuming intracellular GSH [49,50]. AA treatment was cytotoxic toward most of breast cancer cells tested and its higher cytotoxicity compared to DHA was mainly linked to H_2O_2 generation. We identified that proteins involved in DNA replication, cell cycle progression and translations are among the principal targets of AA-induced cysteine redox alterations and could be linked to AA-induced cytotoxicity.

Clinical data demonstrate that plasma VitC concentrations even greater than 10 mM are achievable in humans without causing apparent adverse effects [51,52], and that pharmacological AA are well tolerated by patients and can increase the efficacy of conventional radiotherapy and chemotherapy [15,23]. In our study, such AA concentrations were cytotoxic toward most of breast cancer cell lines without severely affecting normal cells, suggesting that VitC and VitC-based rational drug combinations could be novel therapeutic opportunities for triple-negative breast cancer and other cancers with similar redox properties.

Financial support

This work was supported by the CNRS, the Institut Curie, the Institut National du Cancer SiRIC grant (INCa-DGOS-4645 to MEH), la Fondation ARC grant (PJA 20151203330 to MEH). NEB is supported by PhD program from the Université Paris-Saclay and by the Fondation pour la Recherche Médicale grant (FDT201805005397), EH is supported by a postdoctoral fellowship from the Ligue Nationale Contre le Cancer and Crédit Agricole île de France Mécénat. LV is supported by INSERM.

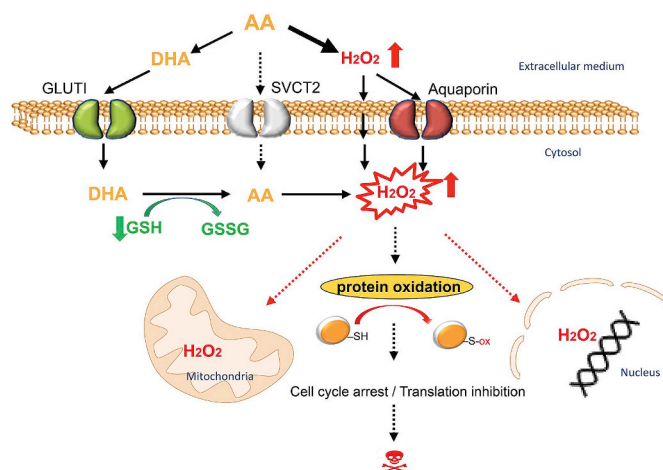


Fig. 8. A model for AA- and DHA-induced cytotoxicity in breast cancer cells. Upon AA-treatment, H_2O_2 is generated in the extracellular medium and then imported to breast cancer cells by aquaporins or by passive diffusion across plasma cellular membranes. Extracellularly generated H_2O_2 appears to be the main source responsible for pro-oxidant properties of AA at pharmacologic concentrations. Although AA may not be imported to cells from the external environment by sodium-dependent VitC transporters (mainly SVCT2) in breast cancer, AA can be oxidized extracellularly into DHA and then imported through glucose transporters (mainly GLUT1). DHA is reduced to AA intracellularly by GSH-dependent mechanisms, consuming intracellular reduced glutathione. AA thus generated further enhances H_2O_2 accumulation in different cellular compartments. A substantial increase in H_2O_2 causes redox modifications of cysteine-containing proteins, including those involved in translation and cell cycle progression. These effects contribute to AA-induced cytotoxicity toward breast cancer cells.

Disclosure of potential conflicts of interest

The authors disclose on potential conflicts of interest.

Acknowledgements

We thank Fabien Reyral and Alice Pinheiro for kindly providing us some of the breast cancer cell lines used. We also thank H el ene Malka-Mahieu, Pierre-Marie Girard, Charl ene Lasgi and Marie-No elle Soler for advice and technical assistance.

Appendix A. Supplementary data

Supplementary data to this article can be found online at <https://doi.org/10.1016/j.redox.2019.101290>.

References

- [1] C. Gorrini, I.S. Harris, T.W. Mak, Modulation of oxidative stress as an anticancer strategy, *Nat. Rev. Drug Discov.* 12 (12) (2013) 931–947.
- [2] D. Trachootham, J. Alexandre, P. Huang, Targeting cancer cells by ROS-mediated mechanisms: a radical therapeutic approach? *Nat. Rev. Drug Discov.* 8 (7) (2009) 579–591.
- [3] L. Chaiswing, W.H. St Clair, D.K. St Clair, Redox paradox: a novel approach to therapeutics-resistant cancer, *Antioxid Redox Signal* 29 (13) (2018) 1237–1272.
- [4] J. Du, J.J. Cullen, G.R. Buettner, Ascorbic acid: chemistry, biology and the treatment of cancer, *Biochim. Biophys. Acta* 1826 (2) (2012) 443–457.
- [5] A.J. Michels, B. Frei, Myths, artifacts, and fatal flaws: identifying limitations and opportunities in vitamin C research, *Nutrients* 5 (12) (2013) 5161–5192.
- [6] Q. Chen, M.G. Espey, A.Y. Sun, J.H. Lee, M.C. Krishna, E. Shacter, P.L. Choyke, C. Pooput, K.L. Kirk, G.R. Buettner, et al., Ascorbate in pharmacologic concentrations selectively generates ascorbate radical and hydrogen peroxide in extracellular fluid in vivo, *Proc. Natl. Acad. Sci. U.S.A.* 104 (21) (2007) 8749–8754.
- [7] Q. Chen, M.G. Espey, A.Y. Sun, C. Pooput, K.L. Kirk, M.C. Krishna, D.B. Khosh, J. Drisko, M. Levine, Pharmacologic doses of ascorbate act as a prooxidant and decrease growth of aggressive tumor xenografts in mice, *Proc. Natl. Acad. Sci. U.S.A.* 105 (32) (2008) 11105–11109.
- [8] M. Levine, M.G. Espey, Q. Chen, Losing and finding a way at C: new promise for pharmacologic ascorbate in cancer treatment, *Free Radic. Biol. Med.* 47 (1) (2009) 27–29.
- [9] K.E. Brandt, K.C. Falls, J.D. Schoenfeld, S.N. Rodman, Z. Gu, F. Zhan, J.J. Cullen, B.A. Wagner, G.R. Buettner, B.G. Allen, et al., Augmentation of intracellular iron using iron sucrose enhances the toxicity of pharmacologic ascorbate in colon cancer cells, *Redox Biol.* 14 (2018) 82–87.
- [10] J. Yun, E. Mullarky, C. Lu, K.N. Bosch, A. Kavalier, K. Rivera, J. Roper, Chio II, E.G. Giannopoulou, C. Rago, et al., Vitamin C selectively kills KRAS and BRAF mutant colorectal cancer cells by targeting GAPDH, *Science* 350 (6266) (2015) 1391–1396.
- [11] C.M. Doskey, V. Buranasudja, B.A. Wagner, J.G. Wilkes, J. Du, J.J. Cullen, G.R. Buettner, Tumor cells have decreased ability to metabolize H₂O₂: implications for pharmacologic ascorbate in cancer therapy, *Redox Biol.* 10 (2016) 274–284.
- [12] S.W. Hong, S.H. Lee, J.H. Moon, J.J. Hwang, D.E. Kim, E. Ko, H.S. Kim, L.J. Cho, J.S. Kang, D.J. Kim, et al., SVCT-2 in breast cancer acts as an indicator for L-ascorbate treatment, *Oncogene* 32 (12) (2013) 1508–1517.
- [13] C. Wohlrab, E. Phillips, G.U. Dachs, Vitamin C transporters in cancer: current understanding and gaps in knowledge, *Front Oncol.* 7 (2017) 74.
- [14] C. Wang, H. Lv, W. Yang, T. Li, T. Fang, G. Lv, Q. Han, L. Dong, T. Jiang, B. Jiang, et al., SVCT-2 determines the sensitivity to ascorbate-induced cell death in cholangiocarcinoma cell lines and patient derived xenografts, *Cancer Lett.* 398 (2017) 1–11.
- [15] J.D. Schoenfeld, Z.A. Sibenaller, K.A. Mapuskar, B.A. Wagner, K.L. Cramer-Morales, M. Furqan, S. Sandhu, T.L. Carlisle, M.C. Smith, T. Abu Hejleh, et al., O₂⁻ and H₂O₂-mediated disruption of Fe metabolism causes the differential susceptibility of NSCLC and GBM cancer cells to pharmacological ascorbate, *Cancer Cell* 32 (2) (2017) 268.
- [16] J.D. Schoenfeld, Z.A. Sibenaller, K.A. Mapuskar, M.D. Bradley, B.A. Wagner, G.R. Buettner, V. Monga, M. Milhem, D.R. Spitz, B.G. Allen, Redox active metals and H₂O₂ mediate the increased efficacy of pharmacologic ascorbate in combination with gemcitabine or radiation in pre-clinical sarcoma models, *Redox Biol.* 14 (2018) 417–422.
- [17] H. Pelicano, D. Carney, P. Huang, ROS stress in cancer cells and therapeutic implications, *Drug Resist Updat.* 7 (2) (2004) 97–110.
- [18] M. Uetaki, S. Tabata, F. Nakasuka, T. Soga, M. Tomita, Metabolomic alterations in human cancer cells by vitamin C-induced oxidative stress, *Sci. Rep.* 5 (2015) 13896.
- [19] Y. Ma, J. Chapman, M. Levine, K. Polireddy, J. Drisko, Q. Chen, High-dose parenteral ascorbate enhanced chemosensitivity of ovarian cancer and reduced toxicity of chemotherapy, *Sci. Transl. Med.* 6 (222) (2014) 222ra218.
- [20] J. Du, J.A. Cieslak 3rd, J.L. Welsh, Z.A. Sibenaller, B.G. Allen, B.A. Wagner, A.L. Kalen, C.M. Doskey, R.K. Strother, A.M. Button, et al., Pharmacological ascorbate radiosensitizes pancreatic cancer, *Cancer Res.* 75 (16) (2015) 3314–3326.
- [21] J. Du, S.M. Martin, M. Levine, B.A. Wagner, G.R. Buettner, S.H. Wang, A.F. Taghiyev, C. Du, C.M. Knudson, J.J. Cullen, Mechanisms of ascorbate-induced cytotoxicity in pancreatic cancer, *Clin. Cancer Res.* 16 (2) (2010) 509–520.
- [22] X. Wei, Y. Xu, F.F. Xu, L. Chaiswing, D. Schnell, T. Noel, C. Wang, J. Chen, D.K. St Clair, W.H. St Clair, RelB expression determines the differential effects of ascorbic acid in normal and cancer cells, *Cancer Res.* 77 (6) (2017) 1345–1356.
- [23] K. Polireddy, R. Dong, G. Reed, J. Yu, P. Chen, S. Williamson, P.C. Violet, Z. Pessetto, A.K. Godwin, F. Fan, et al., High dose parenteral ascorbate inhibited pancreatic cancer growth and metastasis: mechanisms and a phase I/IIa study, *Sci. Rep.* 7 (1) (2017) 17188.
- [24] T. He, E. Hatem, L. Vernis, M. Lei, M.E. Huang, PRX1 knockdown potentiates vitamin K3 toxicity in cancer cells: a potential new therapeutic perspective for an old drug, *J. Exp. Clin. Cancer Res.* 34 (2015) 152.
- [25] P. Liu, H. Zhang, H. Wang, Y. Xia, Identification of redox-sensitive cysteines in the Arabidopsis proteome using OxiTRAQ, a quantitative redox proteomics method, *Proteomics* 14 (6) (2014) 750–762.
- [26] Y. Perez-Riverol, A. Csordas, J. Bai, M. Bernal-Llinares, S. Hewapathirana, D.J. Kundu, A. Inuganti, J. Griss, G. Mayer, M. Eisenacher, et al., The PRIDE database and related tools and resources in 2019: improving support for quantification data, *Nucleic Acids Res.* 47 (D1) (2019) D442–D450.
- [27] D. Graindorge, S. Martineau, C. Machon, P. Arnoux, J. Guittou, S. Francesconi, C. Frochet, E. Sage, P.M. Girard, Singlet oxygen-mediated oxidation during UVA radiation alters the dynamic of genomic DNA replication, *PLoS One* 10 (10) (2015) e0140645.
- [28] E. Hatem, S. Azzi, N. El Banna, T. He, A. Heneman-Masurel, L. Vernis, D. Baille, V. Masson, F. Dingli, D. Loew, et al., Auranofin/vitamin C: a novel drug combination targeting triple-negative breast cancer, *J Natl Cancer Inst.* 111 (6) (2019) 597–608.
- [29] A.J. Meyer, T.P. Dick, Fluorescent protein-based redox probes, *Antioxid Redox Signal* 13 (5) (2010) 621–650.
- [30] V.V. Belousov, A.F. Pradkov, K.A. Lukyanov, D.B. Staroverov, K.S. Shakhbazov, A.V. Tersikh, S. Lukyanov, Genetically encoded fluorescent indicator for intracellular hydrogen peroxide, *Nat. Methods* 3 (4) (2006) 281–286.
- [31] Y.M. Go, D.P. Jones, The redox proteome, *J. Biol. Chem.* 288 (37) (2013) 26512–26520.
- [32] Y.M. Go, J.D. Chandler, D.P. Jones, The cysteine proteome, *Free Radic. Biol. Med.* 84 (2015) 227–245.
- [33] O. Aguilera, M. Munoz-Sagastibelza, B. Torrejon, A. Borrero-Palacios, L. Del Puerto-Nevedo, J. Martinez-Useros, M. Rodriguez-Remirez, S. Zazo, E. Garcia, M. Fraga, et al., Vitamin C uncouples the Warburg metabolic switch in KRAS mutant colon cancer, *Oncotarget* 7 (30) (2016) 47954–47965.
- [34] W.C. Reinhold, M. Sunshine, H. Liu, S. Varma, K.W. Kohn, J. Morris, J. Doroshov, Y. Pommier, CellMiner: a web-based suite of genomic and pharmacologic tools to explore transcript and drug patterns in the NCI-60 cell line set, *Cancer Res.* 72 (14) (2012) 3499–3511.
- [35] U.T. Shankavaram, S. Varma, D. Kane, M. Sunshine, K.K. Chary, W.C. Reinhold, Y. Pommier, J.N. Weinstein, CellMiner: a relational database and query tool for the NCI-60 cancer cell lines, *BMC Genomics* 10 (2009) 277.
- [36] T. He, A. Banach-Latapy, L. Vernis, M. Dardalhon, R. Chanet, M.E. Huang, Peroxiredoxin 1 knockdown potentiates beta-lapachone cytotoxicity through modulation of reactive oxygen species and mitogen-activated protein kinase signals, *Carcinogenesis* 34 (4) (2013) 760–769.
- [37] M. Bajor, A.O. Zych, A. Graczyk-Jarzynka, A. Muchowicz, M. Firczuk, L. Trzeciak, P. Gaj, A. Domagala, M. Siernicka, A. Zagodzkon, et al., Targeting peroxiredoxin 1 impairs growth of breast cancer cells and potentially sensitises these cells to prooxidant agents, *Br J Cancer* 119 (7) (2018) 873–884.
- [38] Q. Chen, M.G. Espey, M.C. Krishna, J.B. Mitchell, C.P. Corpe, G.R. Buettner, E. Shacter, M. Levine, Pharmacologic ascorbic acid concentrations selectively kill cancer cells: action as a pro-drug to deliver hydrogen peroxide to tissues, *Proc. Natl. Acad. Sci. U.S.A.* 102 (38) (2005) 13604–13609.
- [39] M. Levine, S.J. Padayatty, M.G. Espey, Vitamin C: a concentration-function approach yields pharmacology and therapeutic discoveries, *Adv Nutr.* 2 (2) (2011) 78–88.
- [40] E. de Nadal, G. Ammerer, F. Posas, Controlling gene expression in response to stress, *Nat. Rev. Genet.* 12 (12) (2011) 833–845.
- [41] B. Liu, S.B. Qian, Translational reprogramming in cellular stress response, *Wiley Interdiscip Rev RNA* 5 (3) (2014) 301–315.
- [42] D. Silveira, S.C. Formenti, R.J. Schneider, Translational control in cancer, *Nat. Rev. Cancer* 10 (4) (2010) 254–266.
- [43] L.M. Lindqvist, I. Vikstrom, J.M. Chambers, K. McArthur, M. Ann Anderson, K.J. Henley, L. Haplo, L. Cluse, R.W. Johnstone, A.W. Roberts, et al., Translation inhibitors induce cell death by multiple mechanisms and Mcl-1 reduction is only a minor contributor, *Cell Death Dis.* 3 (2012) e409.
- [44] M. Bhat, N. Robichaud, L. Hulea, N. Sonenberg, J. Pelletier, I. Topisirovic, Targeting the translation machinery in cancer, *Nat. Rev. Drug Discov.* 14 (4) (2015) 261–278.
- [45] X. Ren, S.M. Santhosh, L. Coppo, F.T. Ogata, J. Lu, A. Holmgren, The combination of ascorbate and menadione causes cancer cell death by oxidative stress and replicative stress, *Free Radic. Biol. Med.* 134 (2019) 350–358.
- [46] G.P. Bienert, J.K. Schjoerring, T.P. Jahn, Membrane transport of hydrogen peroxide, *Biochim. Biophys. Acta* 1758 (8) (2006) 994–1003.
- [47] H. Tsukaguchi, T. Tokui, B. Mackenzie, U.V. Berger, X.Z. Chen, Y. Wang, R.F. Brubaker, M.A. Hediger, A family of mammalian Na⁺-dependent L-ascorbic acid transporters, *Nature* 399 (6731) (1999) 70–75.
- [48] E. Pena, F.J. Roa, E. Inostroza, K. Sotomayor, M. Gonzalez, F.A. Gutierrez-Castro, M. Maurin, K. Sweet, C. Labrousse, M. Gatica, et al., Increased expression of mitochondrial sodium-coupled ascorbic acid transporter-2 (mitSVCT2) as a central

- feature in breast cancer, *Free Radic. Biol. Med.* 135 (2019) 283–292.
- [49] J.C. Vera, C.I. Rivas, R.H. Zhang, C.M. Farber, D.W. Golde, Human HL-60 myeloid leukemia cells transport dehydroascorbic acid via the glucose transporters and accumulate reduced ascorbic acid, *Blood* 84 (5) (1994) 1628–1634.
- [50] J.M. May, Z.C. Qu, D.R. Neel, X. Li, Recycling of vitamin C from its oxidized forms by human endothelial cells, *Biochim. Biophys. Acta* 1640 (2–3) (2003) 153–161.
- [51] C.M. Stephenson, R.D. Levin, T. Spector, C.G. Lis, Phase I clinical trial to evaluate the safety, tolerability, and pharmacokinetics of high-dose intravenous ascorbic acid in patients with advanced cancer, *Cancer Chemother. Pharmacol.* 72 (1) (2013) 139–146.
- [52] L.J. Hoffer, M. Levine, S. Assouline, D. Melnychuk, S.J. Padayatty, K. Rosadiuk, C. Rousseau, L. Robitaille, W.H. Miller Jr., Phase I clinical trial of i.v. ascorbic acid in advanced malignancy, *Ann. Oncol.* 19 (11) (2008) 1969–1974.